Annales Pharmaceutiques Françaises (2017) 75, 420—435

Disponible en ligne sur ScienceDirect www.sciencedirect.com

Elsevier Masson France EM|consulte www.em-consulte.com

ORIGINAL ARTICLE

Extended stability of the rituximab biosimilar CT-P10 in its opened vials and after dilution and storage in polyolefin bags

Étude de stabilité du biosimilaire du rituximab CT-P10 après ouverture des flacons et après dilution en poches de polyoléfine

V. Vieillard*, M. Paul, T. Ibrahim, A. Astier

UPREC, service de pharmacie, groupe hospitalo-universitaire Henri-Mondor, 51, avenue du Maréchal-de-Lattre-de-Tassigny, 94010 Créteil, France

Received 2 June 2017; accepted 29 June 2017
Available online 4 August 2017

KEYWORDS
Rituximab;
Biosimilar;
CT-P10;
Extended stability;
In-use

Summary The stability of the rituximab biosimilar CT-P10, in 50 mL vials at a concentration of 10 mg/mL, and after dilution to final concentrations of 1 and 4 mg/mL and storage in polyolefin bags at 4 °C and 25 °C was studied by several orthogonal and complementary methods. No significant change (as defined by a magnitude greater than the inter-batch variability) was observed, for each of the parameters characterizing physical and chemical stability studied, for the two concentrations and temperatures tested, or for any of the three batches tested. This implies that cold-chain rupture and exposure to room temperature up to 15 days both for vials and diluted bags have no deleterious consequence on the quality of the product. Moreover, this extended stability permits safe in-advance preparation, dose-banding or flat-dose, that to avoid unnecessary delays in the management of the patient, improvement of the pharmacy and nurse workload and money saving by avoiding non justified losses of this expensive drug.

* Corresponding author.
E-mail address: victoire.vieillard@aphp.fr (V. Vieillard).

http://dx.doi.org/10.1016/j.pharma.2017.06.003

MOTS CLÉS
Rituximab ;
Biosimilaire ;
CT-P10 ;
Stabilité étendue ;
Utilisation d'usage

Résumé La stabilité du rituximab biosimilaire CT-P10, en flacons de 50 mL à une concentration de 10 mg/mL, et après dilution à des concentrations finales de 1 et 4 mg/mL et stockage dans des poches en polyoléfine à 4 °C et 25 °C, a été étudié par plusieurs méthodes orthogonales et complémentaires. Aucun changement significatif (tel que défini par une variation supérieure à la variabilité inter-lot) a été observé, pour chacun des paramètres caractérisant la stabilité physique et chimique étudiée, pour les deux concentrations et les températures testées, ou pour l'un des trois lots testés. Cela implique que la rupture de la chaîne du froid et l'exposition à la température ambiante jusqu'à 15 jours n'ont aucune conséquence délétère sur la qualité du produit. En outre, cette stabilité prolongée permet sans danger une préparation anticipée, un dose-banding ou une dose unique standardisée, ceci pour éviter des retards inutiles dans la prise en charge du patient, l'amélioration de la charge de travail de la pharmacie et de l'infirmière et des économies substantielles en évitant des pertes non justifiées de ce médicament coûteux.

Introduction

Rituximab (RTX) is a chimeric monoclonal antibody (mAb) indicated in non-Hodgkin's lymphoma [1], rheumatoid polyarthritis [2] and chronic lymphoid leukemia. It acts against CD20, which is expressed in all the B-cell lines, and thus, induces a depletion of CD20-positive cells [3]. Because of its proteic nature, RTX may go through a variety of chemical and physical degradation processes, as recently reviewed by Manning [4]. Physical instability mostly concerns low energy bonds (such as hydrogen bonds), and includes adsorption on to surfaces, unfolding and aggregation [5—7]. Chemical instability, such as asparagine deamidation (the most common chemical degradation process), aspartic acid isomerization, oxidation or disulfide bond shuffling, concerns covalent bond modifications [7,8]. Many stress factors are routinely encountered during the preparation, purification, shipping or storage of protein products and especially mAb [9]. Since several years, biosimilars of therapeutic proteins are available in EU, mainly growth factors such as erythropoietin and G-CSF. Very recently, the first biosimilar of RTX has been registered in EU one year after the mAb infliximab (CT-P10; manufactured by Celltrion, South Korea, and marketed in France by Biogaran). In a previous work, we have demonstrated that the princeps of RTX (MAbthera®, Roche laboratories, France) was very stable after dilution and storage in polyolefin bags, both at 4 °C and 22 °C [10]. This finding permits us to manufacture batches of a flat-dose of 600 mg RTX in bags in order to improve pharmacy workload and the patient's care and also to save money by avoiding unjustified losses of this expensive product.

No public data comparing the physicochemical properties of CT-P10 data with its princeps is available However, biosimilars marketed in E.U. were evaluated by a fully comparative exercise to obtain their marketing authorization The primary, secondary, and higher-order structure, post-translational modifications, glycosylation, charge variants, purity/impurities, quantity and biological properties were elucidated using orthogonal analytical techniques. Minor variations in terms of charge and glycosylated variants can be observed between princeps and biosimilars but without consequence on biological activity and toxicity.

Thus, since a biosimilar was highly comparable to its princeps, it is likely to consider that its stability was also comparable. However, the extensive comparability exercise required to obtain marketing authorization does not include extended stability data (in-use stability). Therefore, it is crucial for the users to be sure that a biosimilar exhibits the same extended stability that its princeps.

The stability of the rituximab biosimilar CT-P10, in 50 mL vials at a concentration of 10 mg/mL, and after dilution to final concentrations of 1 and 4 mg/mL and storage in polyolefin bags at 4 °C and 25 °C was studied by several orthogonal and complementary methods as recommended [9,11].

Material and methods

Reagents

Disodium hydrogen phosphate, sodium azide, potassium dihydrogen phosphate were purchased from Merck (Darmstadt, Germany). Acetonitrile for HPLC and MES (2-(N-Morpholino) ethanesulfonic acid) were obtained from Sigma—Aldrich (St Louis, MO, USA). Isotonic saline (batch13KIS24; expiry date: 09/2018) was provided by Fresenius Kabi (Louviers, France). All reagents were of analytical grade.

CT-P10, 50 mL vials at 10 mg/mL, was a gift from Biogaran (France). To test the batch variability, and to estimate the acceptable range for each quality attribute, 3 different batches were used (Batch 1: 15C2C03; Batch 2: 15C2C08; Batch 3: 15C2C10).

For several experiments, the analytical samples were diluted in a dilution buffer (20 mM KH_2PO_4, pH 6.0, filter-sterilized on a 0.22 μm-pore filter).

Preparation of the trial bags

Under laminar flow hood and following strict and validated aseptic techniques, we prepared 12 bags. Three bags at concentration C1 (1 mg/mL) for storage at 4 °C (corresponding to batches 1 to 3) labeled C1-4; 3 bags at concentration

C2 (4 mg/mL) for storage at 4 °C (corresponding to batches 1 to 3) labeled C2-4; 3 bags at concentration C1 for storage at 25 °C (corresponding to batches 1 to 3) labeled C1-25, and 3 bags at concentration C2 for storage at 25 °C (corresponding to batches 1 to 3) labeled C2-25.

For the preparation of bags of solution with a concentration of 1 mg/mL, we introduced 5 mL of the pure product (a 10 mg/mL solution) into a 50 mL bags from which the NaCl had been removed, and we then made the volume up to 50 mL with 0.9% NaCl.

For the bags of solution at 4 mg/ml, we introduced 20 mL of the pure product into the pouch with 30 mL of 0.9% NaCl, as described above. This method was followed to overcome the theoretical volume variation problems frequently encountered with solute bags. The weights of the different bags were very similar, with no significant differences detected on Anova, demonstrating a high level of homogeneity between preparations.

The trial bags and vials were then stored at 4 °C in a certified refrigerator (temperature range: +2 to +4 °C) or in a air conditioned room (21—25 °C) the temperature in the two storage facilities being recorded continuously by the SIRIUS® system. The bags were stored in an opaque sachet to assure complete darkness. The vials were also stored in complete darkness, with the sampling device guaranteeing sterility left in place.

Samples for analysis

Once the bags had been prepared, a 7 mL sample was removed from each bag with a syringe for the initial reference determinations (T0). After sampling, the bags were reweighed to determine their initial weight for the calculation of water loss during storage. They were then placed in the appropriate storage conditions. We removed a 2 mL sample from each vial for all the analyses. The pure product (10 mg/mL solution) was diluted, if necessary, for analyses in the same conditions as for the bags. Samples taken after 7, 14 and 28 days are named in the text as D7, D14 and D28 respectively.

Analyses performed

The methods were previously validated as stability-indicating during our previous study on the stability of RTX princeps and several mAbs such as trastuzumab and ipilimumab [10,12,13].

Spectroscopic and turbidity determinations

All analysis were performed using a UV spectroscopy, turbidimetry: Cary 50 Probe, Varian, Inc., Palo Alto, USA, 1 cm quartz micro-cuvettes. Turbidity analyses were performed on pure samples. For measurements at 279 nm, before and after centrifugation (Sigma® benchtop centrifuge; 12,000 × g for 5 min), the samples were diluted to 0.4 mg/mL in dilution buffer. A scan was performed between 200 and 600 nm, for each sample before and after centrifugation, against the blank at a rate of 200 nm/min. The respective absorbances at 279 and 350 nm were determined from the spectrum. The second derivative of the spectrum between 250 and 320 nm was analyzed.

Turbidimetry

This method was used to estimate the amounts of visible protein aggregates, through the measurement of optical density at 350 nm. The intrinsic chromophores of the protein do not absorb at this wavelength. Only aggregates in suspension diffract the incident light, causing an opalescence and resulting in pseudo-absorbance [14]. This method does not permit evaluation of the size of aggregates. Thus, this method should be used only in comparative measurements such as modifications of turbidity over time in stability programs, 2-4-1-2-UV spectrometry at 279 nm.

UV spectroscopy can be used to detect sub-visible aggregation through the aggregation index [15] (equation no. 1). After centrifugation, any variation absorbance at 279 nm provides evidence of a loss of protein during storage, through adsorption to surfaces or aggregation.

Equation 1: aggregation index formula

$$AI = \frac{OD_{350}}{OD_{279} - OD_{350}} \times 100$$

AI = aggregation index; OD_{279} = optical density at 279 nm; OD_{350} = optical density at 350 nm.

Second derivative UV spectroscopy

This method can be used to evaluate the impact of dilution and storage on the aromatic amino acids of the molecule. The position of the absorbance peaks on the second derivative spectrum is sensitive to the polarity of the microenvironment of these amino acids and can therefore provide an overall vision of the tertiary structure of the molecule [16]. The spectrum was analyzed between 250 and 320 nm. The data were unsmoothed and the derivate spectra were obtained using a 9 points algorithm. The operating conditions were identical to those used for ratio determinations on D0. Five major peaks (252-Phe, 258-Phe, 275-Tyr, 284-Thy/Trp and 292-Trp), were monitored, together with two minima, at 287 and 295 nm [16,17].

Fluorescence spectroscopy

The possible modifications of the tertiary structure during storage were estimated by fluorescence spectrometry. Indeed, fluorimetry may be used through direct (intrinsic) fluorescence of the aromatic amino acids: phenylalanine, tyrosine and mostly tryptophan, absorbing UV respectively to 257 nm, 275 nm and 280 nm [18]. Samples diluted in the dilution buffer were excited at 279 nm at 25 °C and the emission spectra were recorded between 310 and 410 nm (Perking Elmer fluorimeter).

Ion-exchange chromatography (IC)

The charge variants were analyzed by weak-cation exchange gradient chromatography [12,19]. Samples were injected pure or diluted to a concentration of 1 mg/mL in dilution buffer. An excipient blank was used to check for the absence of interference (Sodium citrate. 2 H_2O: 377.5 mg NaCl: 450 mg; 35 mg polysorbate 80; HPLC grade water QS 50 mL; filtered at 0.22 μm). The mobile phases consisted in a phase A: (20 mM MES and 60 mM NaCl; pH 6.0) and a phase B (20 mM MES and 180 mM NaCl; pH 6.0) both in HPLC grade water, filtered at 0.22 μm and degassed by ultrasound. A biocompatible Thermo Scientific Ultimate 3000 HPLC system

consisting of an ISO-3100 SD pump, a WPS-3000 automatic injector and an UV multi-wavelength 3000 detector was used. A Propac® WCX-10 column (4 × 250 mm) fitted to a Propac WCX 10G pre-column, both maintained at 35 °C, was used at a low rate of 0.8 mL/min. Samples of 100 μL were injected and the peaks were detected at 280 nm.

The samples were analyzed by a 60-min salt gradient (initial composition of the mobile phase: 45% A and 55% B followed by a linearly increase in 40 min to 100%; B then returning in 10 min and maintained up to 10 min at the initial composition).

Size-exclusion chromatography SEC

The evaluation of dimers, trimers and high-molecular weight species (HMW) and molecule fragmentation was performed by SEC [19] using the same chromatographic system than for IC but the detection was made using a FLD-3000 RS fluorescence detector (Excitation at 280 nm, emission at 335 nm). The mobile phase was 0.2 M K_2HPO_4, 0.25 M KCl and 0.05% NaN_3 in HPLC grade water, adjusted at pH 7.0 with 1 M H_3PO_4 and filtered at 0.22 μm. After centrifugation (15,000 × G for 5 min) the samples were diluted at the required concentration by the dilution buffer and 100 μL were injected onto a Yarra 3000 Phenomenex® (300 × 7.8 mm) column protected with a Phenomenex security guard GFC3000® (4 × 3 mm) pre-column (room temperature). The flow rate was a 0.6 mL/min. A reconstituted excipient solution was used as blank.

Dynamic light scattering

Submicron particles

Dynamic light scattering (DLS) is a sensitive method for evaluating the size of populations of molecules, oligomers and aggregates from 1 nm to 6 μm in size. It measures the Brownian motion of the particles, which it links to their size. A Malvern Zetasizer Nano ZS (Worcestershire, UK) laser light scattering system was used to obtain DLS measurements with a 633 nm laser source. The NanoZS® software was used for data acquisition and analysis. We analyzed in triplicate 200 μL of each undiluted sample in a quartz micro-cuvette previously rinsed with injection-grade water (0.22 μm-filtered). All these steps were performed in a laminar flow hood, to prevent contamination with external particles. The size and distribution of the hydrodynamic diameters of the antibodies and small aggregates (100 to 1000 nm) were determined, together with their dispersity indices (DI), for the estimation of dimerization rates, by integrating the measured intensity of scattered light.

Thermal aggregation curve (thermodynamic stability)

During temperature increases, dilution/concentration effects, or simply during long-term storage, the high-order structures (secondary, tertiary and quaternary) of proteins may change, signaling unfolding of the protein and, subsequently, aggregation, due to an increase in the exposure of hydrophobic surfaces [5,7,18]. These events can be observed by DLS, because they lead to major changes in protein size during denaturation. By gradually increasing the temperature (1 °C/min, with three minutes of equilibration between steps) from 55 to 78 °C, and measuring hydrodynamic diameter at each temperature, the thermal aggregation curve can be plotted. The temperature of aggregation (Tagg), at which the aggregated fraction is 0.5 during thermal transition, can be determined using the nonlinear least squares method to fit the diameter dependence on the temperature to a sigmoidal model (Kaleidagrah® software). The thermodynamics parameters were calculated as previously by Farruggia et al. [20]. A comparison of the curves obtained for each storage duration and temperature can be used to estimate slight overall destabilization of the three-dimensional structure by energy accumulation that could not be detected by the other methods, which detect only already denatured states.

Estimation of the quinary structure by SEC

The measurement of retention times by SEC as a function of the concentration of the protein in solution (injection-dilution SEC) can be used to assess quinary structure which can estimate the tendency of the protein to form oligomers [21]. Indeed, the dependence of SEC retention volume or Tr on injection mass and molecular shape is well-known in protein biochemistry [22].

Dilutions (0.05 to 10 mg/mL) of rituximab biosimilar were analyzed by SEC, as described at the previous paragraph. The retention time (Tr) were determined and plotted as the Tr = f(conc) curve. An absence of quinary structure is characterized by a curve in which Tr varies very little as a function of concentration (typically < 0.10 min for a dilution factor of 20). In the opposite, for mAb having strong tendency to oligomerization such as for infliximab, a steep curve is observed with a decrease of Tr > several minutes over the range of dilution [23].

General properties

Several general properties (density, osmolarity and pH) of the CT-P10 solutions were determined as a function of storage conditions.

Density

Density of undiluted samples was measured by the oscillating U-tube method, at 25 °C (DMA 35 Anton PAAR portable) densimeter.

pH

An electronic pH meter with a glass combination microelectrode was used (Consort P901 pH meter, Bioblock Scientific). The pH meter was calibrated before each series of measurements. The precision of measurements was 0.01 pH unit. The pH values were expressed at 25 °C (application of temperature correction).

Osmolarity

Osmolarity was measured on a volume of 100 μL, by the freezing point depression method with calibration against a 300 mOsmole standard (Hermann Roebling automatic micro-osmometer, model: 12/12DR).

Sterility test

Sterility tests were performed on the four bags for each batch, after pooling, and on the leftover material in the vials

Table 1 Mean turbidity between concentrations at 350 nm (mean ± SD of 3 batches).
Turbidité moyenne à 350 nm entre les concentrations (moyenne ± SD de 3 lots).

Temp (°C)	Time	C1 (1 mg/mL)		C2 (4 mg/mL)	
		T0	D28	T0	D28
4 °C	Mean	0.04287	0.04230	0.05473*	0.05481
	Median	0.04185	0.04182	0.05474*	0.05482
	SD	0.00304	0.00077	0.00031	0.00311
25 °C	Mean	0.04287	0.04247	0.05473*	0.05493
	Median	0.04185	0.04248	0.05474*	0.05439
	SD	0.00304	0.00051	0.00058	0.00042

* $P < 0.0002$ vs. 0.7 mg/mL.

for the three batches. Sterility tests were performed on D28 samples only since they represent the higher risk of contamination. These tests were performed with Millipore Steritest Symbio Pumps, based on the membrane filtration technique. The two culture media used were thioglycolate medium (incubated at 32 °C) and casein and soy hydrolysate medium (incubated at room temperature). The cultures were incubated for 14 days and the absence of microbial growth was checked by comparing the cloudiness of the medium with that of a negative control.

Search for large particles by microscopy

The aim was to check for the presence of particles of 10 to 50 μm in diameter in the stability test samples. The samples were prepared in a laminar flow hood to prevent external contamination, and 50 μL of the sample was then introduced into a hemocytometer covered with a slide. All the material used was rinsed before use with injection-grade water filter-sterilized with a 0.22 μm-pore filter, and left to dry under laminar flow. The images were recorded and analyzed by an Olympus IM inverted microscope (Olympus SA, Rungis, France) equipped with a color camera (XCD-U1000 CR; 1600 × 1200 pixels, Sony, Japan), and image analysis software (Ellix, Microvision Instruments, Evry, France).

Analysis of results

Samples were analyzed in triplicate. Statistical analyses were performed by parametric testing. Comparisons were performed by the student *t*-test, Anova, or Student-Newman-Keuls multiple comparison test as appropriate. The assumption of normal distribution was first tested by an F-test. Differences were only considered to significant for $P < 0.01$, which is stricter than the usual significance set at 0.05, because of the analytical variability of the analyses, notably chromatographic, observed during the triplicate measurements (< 2%) and the inherent imprecision of the integration processes, particularly for small areas.

The weights of the different bags were very similar with no significant differences by Anova, showing excellent homogeneity of the preparations (range: 59.27—59.79 g; max CV < 1%). The conservation temperatures of +4 and +25 °C remained within the acceptance limits for the duration of the study.

Results and discussion

Turbidity and absorbance

Turbidity

For each point, determined in triplicate, variation between measurements was very low, typically below 0.001 OD units (1 mOD unit). The mean turbidity at T0 for the three batches was 42.87 ± 2.7 mOD units and the median value was 41.85 mOD units, demonstrating little inter-batches variability. The values followed a Gaussian distribution. As expected, mean turbidity was higher for 4.0 mg/mL rituximab biosimilar than for 1.0 mg/mL rituximab biosimilar (about +12 mOD units; $P < 0.0002$; Table 1). We noted no change in turbidity at 350 nm after 28 days of storage, with no difference as a function of concentration, batch or temperature. These results demonstrate the absence of light-diffracting aggregate formation during the 28-day storage period, whether at +4 °C or at +25 °C, after dilution in bags.

For the vials, as expected, turbidity was higher than in the bags, due to the higher concentration of the solution. A slight difference between batches was observed, with a maximum variation of 8.1 mDO units. We observed no significant change in turbidity as a function of storage time at 4 °C. However, for storage at 25 °C, a small but significant increase in turbidity was observed only for batch 2 (+4.18 mDO units). No change in turbidity was observed for batches 1 and 3. However, the increase observed for batch 2 remained within the limits of inter-batch variability (Table 2) and the gradient of a plot of the means vs. time was not significantly different from zero demonstrating thus the absence of aggregation vs. time for the vials. These findings are in excellent accordance with the results observed with the bags.

Absorbance at 279 nm

Mean absorbance at 279 nm at T0, just after dilution, was 0.6377 ± 0.0157 OD unit for all the prepared bags (C1 = 1 mg/mL: 0.6262 ± 0.010; C2 = 4 mg/mL: 0.6492 ± 0.0109 OD unit). These results confirm the homogeneity of the content of the three batches tested and of the final preparations. After 28 days of storage, mean absorbance at 279 nm was 0.6244 ± 0.0027 OD unit for the

Table 2 Changes in turbidity at 350 nm from T0 to D28 for each batch expressed in mDO units. Mean ± SD ($n = 3$ for each batch).
Modifications de la turbidité de T0 à T28 jours pour chaque lot, exprimée en unité mDO. Moyenne ± SD ($n = 3$ pour chaque lot).

	Batch 1	Batch 2	Batch 3	Maximum absolute variation between batches
T0				
Mean	79.07	78.92	82.73	8.10
SD	1.08	0.28	0.98	
D28 4 °C				
Mean	75.70	78.38	78.90	3.19
SD	3.04	0.51	0.58	
D28 25 °C				
Mean	80.10	83.10*	83.57	8.47
SD	0.07	0.05	0.03	
Change from T0 to D28	+1.03	+4.18	+0.084	

* $P > 0.01$.

C1 bags stored at 4 °C (non- significant difference relative to T0), and 0.6419 ± 0.0011 OD unit for the C1 bags stored at 25 °C (non-significant difference relative to T0). Similar results were obtained for the C2 bags (Table 3).

We observed no significant variation, for either concentration, as a function of the time or temperature of storage (ANOVA with an alpha risk of 0.05: $P = 0.16608$; Student-Newman-Keuls multiple comparison test: no significant difference, with *P*-values of 0.3736 to 0.9999). We can conclude that there was no protein loss, by adsorption in particular, during storage, whatever the concentration and storage temperature.

The aggregation indexes (AI) at T0 are < 0.1, indicating a low aggregation level. AI is slightly higher for the 4 mg/mL bags than for 1 mg/ml bags due to the initial higher turbidity. However, for each concentration and storage temperature, the respective aggregation index at D28 was not different from T0. This result confirms that no significant aggregation, estimated by opalescence at 350 nm, occurs during storage, regardless of the concentration and temperature.

Derivative UV and fluorescence spectrometry: tertiary structure

Second derivative spectrometry analysis of the UV spectrum zone corresponding to aromatic amino acids (260—300 nm) was performed to assess changes in the tertiary structure of the antibody during storage. The position of the absorbance peaks on the second derivative of the spectrum is sensitive to the polarity of the microenvironment of these amino acids and can thus provide an overall vision of the tertiary structure of the molecule. We analyzed the spectrum between the wavelengths of 250 and 320 nm. The operating conditions were identical to those used to measure optical density. Five major peaks were followed (252-Phe, 258-Phe, 275-Tyr, 284-Thy/Trp and 292-Trp), together with two

Table 3 Absorbance at 279 nm (DO unit) vs. time as a function of storage temperature for both concentrations (mean ± SD of 3 batches) and aggregation index (as defined in equation 1) at T0 and after 4 weeks of storage. No significant difference was observed.
Absorbance à 279 nm (unité DO) vs temps en fonction de la température de stockage pour les 2 concentrations (moyenne ± SD de 3 lots) et index d'agrégation (comme défini à l'équation 1) à T0 et après 4 semaines de stockage. Aucune différence n'a été observée.

Time	C1 (1 mg/mL)				C2 (4 mg/mL)			
	4 °C		25 °C		4 °C		25 °C	
	Mean	SD	Mean	SD	Mean	SD	Mean	SD
TO	0.6262	0.0034	0.6492	0.0109	0.6439	0.0047	0.6546	0.0070
D7	0.6349	0.0029	0.6388	0.0011	0.6434	0.0051	0.6498	0.0059
D14	0.6064	0.0023	0.6398	0.0051	0.6271	0.0053	0.6483	0.0023
D21	0.6156	0.0012	0.6517	0.0088	0.6455	0.0045	0.6518	0.0139
D28	0.6244	0.0027	0.6419	0.0011	0.63683	0.0100	0.6598	0.0057
Aggregation index								
TO	0.0735	0.0004	0.0958	0.0016	0.0707	0.0005	0.0921	0.0010
D28	0.0727	0.0003	0.0934	0.0002	0.0710	0.0006	0.0908	0.0008

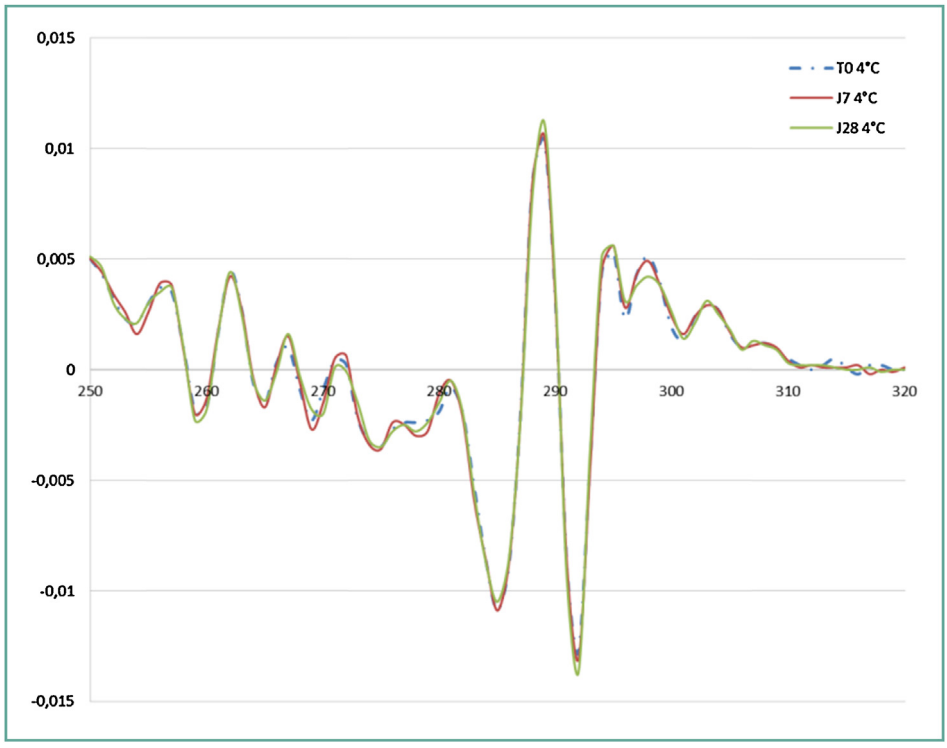

Figure 1. Second derivative of the UV spectrum of the rituximab biosimilar after storage at 4 °C. No change was observed, even after 28 days of storage.
Spectres UV en dérivé seconde du rituximab biosimilaire après stockage à +4 °C. Aucune modification n'est observée, même après 28j de stockage.

minima at 287 and 295 nm. Fig. 1 shows that the tertiary structure of the antibody remained completely unchanged after storage at 4 °C for 28 days. By contrast, after storage at 25 °C for 28 days, we observed small discrepancies, particularly for the peaks at 269, 296 and 301 nm, which displayed a red shift of 1 to 2 nm (Fig. 2). The observed changes in the 250—270 nm region can be attributed to changes in the environment of the phenylalanine molecule

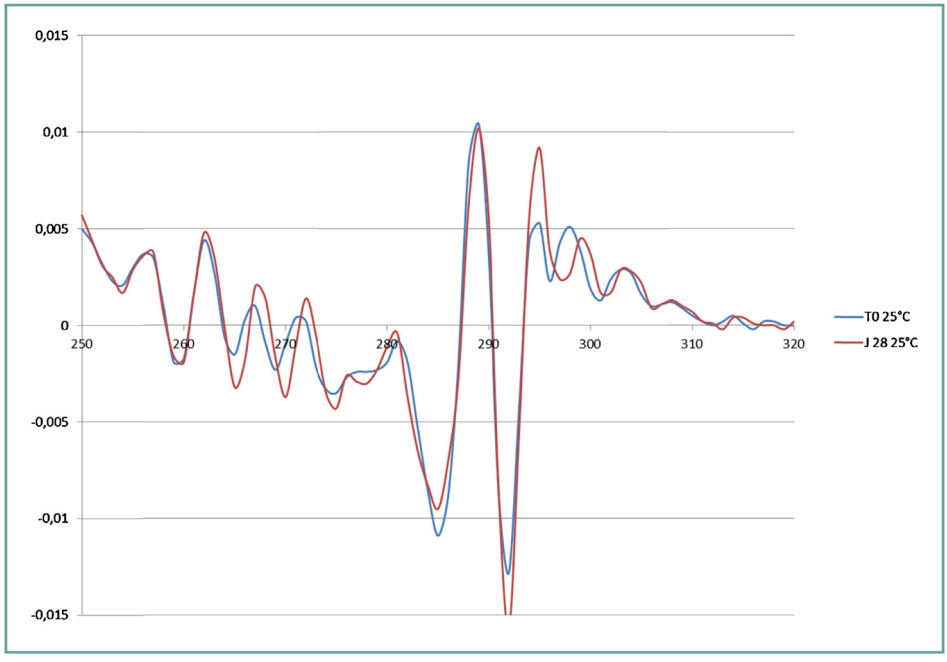

Figure 2. Second derivative UV spectrum of the rituximab biosimilar at T0 and after storage at 25 °C for 28 days. Some shifts are noticed.
Spectres UV en dérivé seconde du rituximab biosimilaire à T0 et après stockage à 25 °C pendant 28 jours. Des déplacements de pics sont notés.

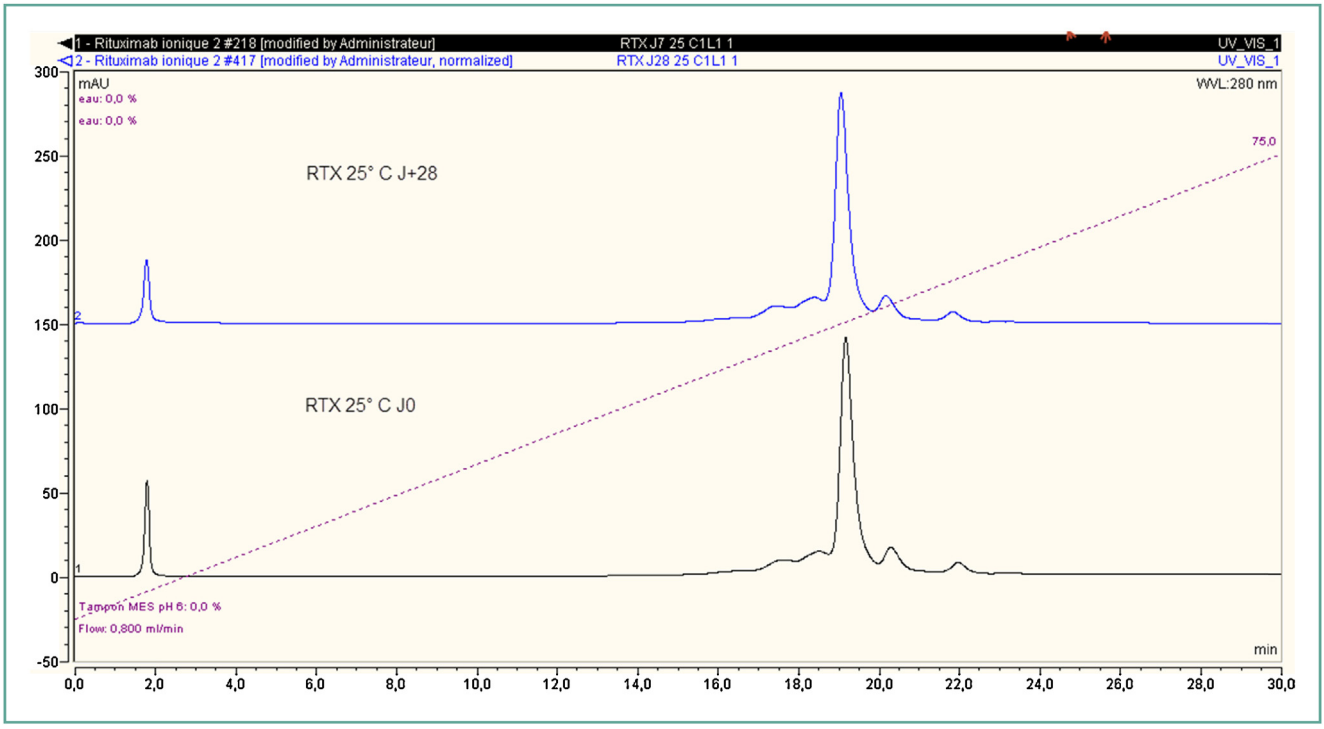

Figure 3. Typical ion-exchange chromatography profiles of the rituximab biosimilar at T0, and after storage for 28 days at 25 °C after dilution to 4 mg/ml in a bag. No difference was observed.
Chromatogramme typique par échange d'ions du rituximab biosimilaire à T0, après stockage 28 jours à 25 °C, et après dilution à 4 mg/mL en poche. Aucune différence n'est observée.

due to exposure to water during the unfolding of the initially folded structure. Similarly, the red shifts between 290 and 300 nm, but without a shift of the peaks at 292 nm, are consistent with a change in the environment of tyrosine residues in the absence of a change in the environment of tryptophan residues. These results are consistent with those of our previous study on the stability of Mabthera® rituximab, which showed the same shifts in the peaks at 269, 296 and 301 nm but after six months of storage at 4 °C.

The fluorescence emission spectra had an identical profile, with emission peaks that did not vary with duration of storage. We observed non-significant variations of intensity that could be attributed to the intrinsic variability of the method (successive dilutions). These results confirm the absence of change in the microenvironment surrounding the tryptophan residues.

We can therefore conclude that storage of the rituximab biosimilar at 25 °C for 28 days triggers a change in tertiary structure, with the exposure of a region containing phenylalanine and tyrosine residues, but not tryptophan residues. No such change is observed after storage at 4 °C.

Ion-exchange chromatography

The pH gradient method demonstrated the presence of seven rituximab charge variants numbered 1 to 7. The variant 4 predominated, accounting for a mean of about 86% of the molecules present (Fig. 3). This variant is described as ''0K'', corresponding to an isoform with C-terminal lysine residues missing from the heavy chain, but with N-terminal pyroglutamic acid residues [23]. We identified three acidic variant peaks corresponding to deaminated, sialated and glycanated protein species (about 2.5% in total), and three basic variant peaks (about 11%) in good accordance to Viser et al. [23]. No significant difference in profile was observed between the three batches tested. The area under the curve (AUC) was determined by peak integration. The relative percentage of the total AUC corresponding to each peak was determined for each concentration, batch, temperature, and storage duration. For the small peaks (< 2%; peaks 1, 2, 3 and 7), the analytical variability of integrations within batches ($n = 12$; each point in triplicate for T0) was of the order of 10%. It was about 2.5% for peaks 5 and 6, and less than 0.2% for the principal peak (peak 4). Anova and Student-Newman-Keuls multiple comparison tests revealed no significant differences, at T0, in the percentages of the ionic variants between batches and concentrations.

Changes during storage: Fig. 3 shows a typical chromatogram for 4 mg/mL solution prepared in bags, at T0 and after 28 days of storage at 25 °C. More detail is provided in Fig. 4. No new peak, in either the acidic or basic part of the chromatograms, potentially corresponding to new degradation products, due to the deamidation of asparagine residues, for example, was observed. However, we did note a very slight change in the relative percentages of the charge variants after 28 days of storage at 25 °C, whereas no change was observed after storage at 4 °C (Table 4). We noted a slight increase in the acidic variants corresponding to peaks 2 and 3, for both concentrations. A concomitant decrease of the principal peak was observed for 1 mg/mL concentration, but not for 4 mg/mL without clear explanation for this difference.

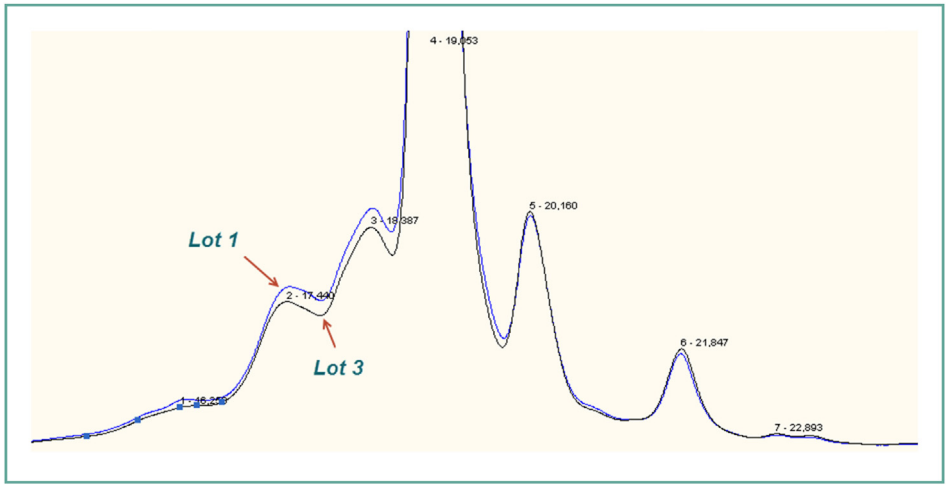

Figure 4. Details of the ion-exchange chromatography profile, showing the seven peaks corresponding to variants in two different batches. Batch 1 contains a higher percentage of acidic variants than batch 3 (peak 2: 1.88% vs. 1.03%; peak 3: 1.76% vs. 0.76%).
Détails du profil chromatographique en échange d'ions montrant les 7 pics correspondants aux variants dans 2 lots différents. Le lot 1 contient un pourcentage plus élevé de variants acides que le lot 2 (pic 2 : 1,88 % vs 1,03 % ; pic 3 : 1,76 % vs 0,76 %).

For vials, no change in chromatographic profiles or the relative percentages of variants was observed after storage at 4 °C or 25 °C (data not shown).

Overall, the data from ionic chromatography demonstrate the excellent stability of the rituximab biosimilar in vials and after dilution to two concentrations in bags, after one month of storage at 4 °C or 25 °C.

Size-exclusion chromatography (SEC)

SEC was used to visualize the monomer of the rituximab biosimilar and possible oligomers (dimers or trimers), together with high-molecular weight polymers indicative of the start of aggregation that might ultimately lead to the formation of submicron- and then micro-sized aggregates. This method can also be used to demonstrate intra- or extracatenary fragmentation, such as heavy and light chains forming compounds with a lower molecular weight through the cleavage of disulfide bridges at the hinge. Fig. 5 shows an example of a chromatogram for T0 and D28, with a magnification showing the dimer and HMW peaks in Fig. 6.

Table 5 shows the relative percentages of each peak relative to various experimental conditions. At T0, following dilution in the bags, the rituximab biosimilar yielded four peaks, one of which was much more prevalent than the others (monomer: 99.476 ± 0.176%; range: 98.92–99.55%). On

Table 4 Changes in the relative percentages of the charge variants of the rituximab biosimilar diluted in bags, after 28 days of storage (mean ± SD of 3 batches for 2 concentrations and 2 temperatures).
Modifications des pourcentages relatives des variants de charge du rituximab biosimilaire dilué en poches, après 28 jours de stockage (moyenne ± SD de 3 lots pour 2 concentrations et 2 températures).

	Variant no.	T0				D28				Difference relative to T0 for storage at 25 °C
		4 °C		25 °C		4 °C		25 °C		
		Mean	SD	Mean	SD	Mean	SD	Mean	SD	
C1	1	0.290	0.053	0.297	0.038	0.320	0.030	0.317	0.028	NS
	2	1.74	0.095	1.457	0.023	1.753	0.026	2.020	0.045	< 0.05
	3	0.909	0.042	1.243	0.044	1.390	0.182	1.957	0.096	< 0.05
	4	86.643	0.119	86.640	0.201	87.147	1.270	82.880	0.587	< 0.05
	5	6.457	0.274	6.290	0.191	6.627	0.158	6.420	0.318	NS
	6	3.688	0.068	4.107	0.038	4.013	0.098	3.657	0.038	NS
	7	0.280	0.030	2.070	0.003	0.267	0.038	0.207	0.009	NS
C2	1	0.370	0.037	0.277	0.041	0.483	0.021	0.340	0.047	NS
	2	1.757	0.072	1.697	0.135	1.770	0.077	2.283	0.014	< 0.05
	3	0.870	0.085	1.030	0.117	1.360	0.123	2.117	0.059	< 0.05
	4	86.697	0.256	86.440	0.228	87.003	0.138	86.753	1.940	NS
	5	5.443	0.214	8.460	0.275	6.623	0.251	6.803	0.172	NS
	6	3.710	0.082	3.760	0.188	3.930	0.059	3.337	0.103	NS
	7	0.260	0.052	0.271	0.038	0.273	0.034	0.190	0.006	NS

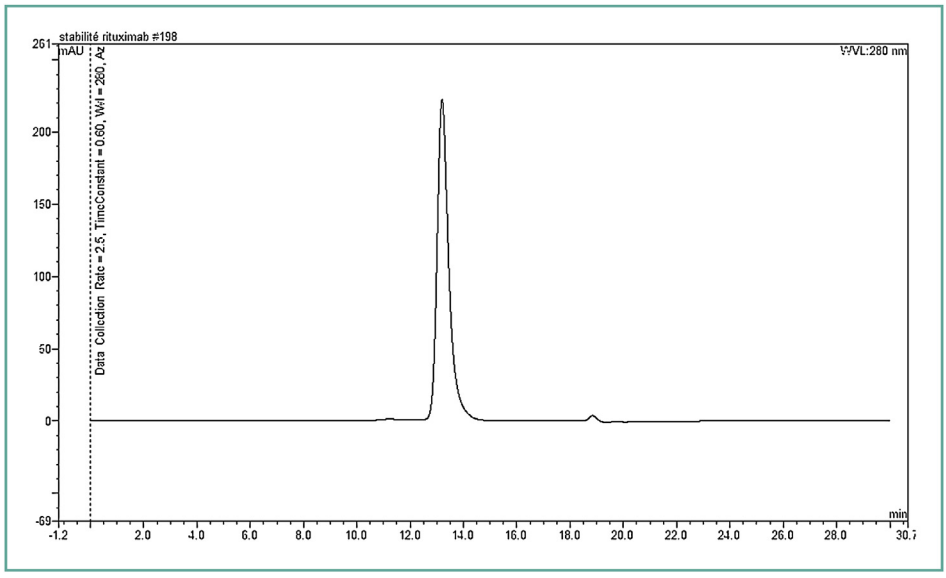

Figure 5. Typical SEC chromatogram for the rituximab biosimilar.
Chromatogramme SEC typique du rituximab biosimilaire.

average, 0.293 ± 0.021% corresponded to a peak considered to represent a HMWP, and 0.096 ± 0.005% corresponded to a dimer. No difference was found between the results for the two concentrations. There was also a peak corresponding to a component with a lower molecular weight, corresponding to about 0.08%.

In vials at T0, the monomer accounted for 98.828 + 0.070% ($P < 0.01$ vs. diluted solutions) of the molecules present, with no difference between the percentages obtained for the undiluted solution in vials and the diluted solution in bags for the dimer (0.098 ± 0.002%) and HMW (0.283 ± 0.008) peaks. The percentage for the low-molecular weight peak was higher in the vials than in diluted solutions, at 0.789 ± 0.070%. In vials on D28, the monomer accounted for 99.055 ± 0.011 of the molecules present (non-significant difference relative to T0). We observed a slight decrease in dimer levels (0.092 + 0.004%; $P < 0.05$), with no change in the oligomer peak. The peak for the low-molecular weight for decreased slightly, to 0.592 ± 0.028% ($P < 0.05$). No additional peaks were detected at D28, demonstrating the absence of oligomer formation and modification of the molecule that might lead to fragmentation, for both the diluted solutions and for the undiluted solution in the vials.

No significant differences in AUC were observed (ANOVA and Student-Newman-Keuls multiple comparison tests), regardless of concentration, batch, temperature or duration of storage, consistent with the results of UV spectroscopy at 279 nm and ion-exchange chromatography. The variations

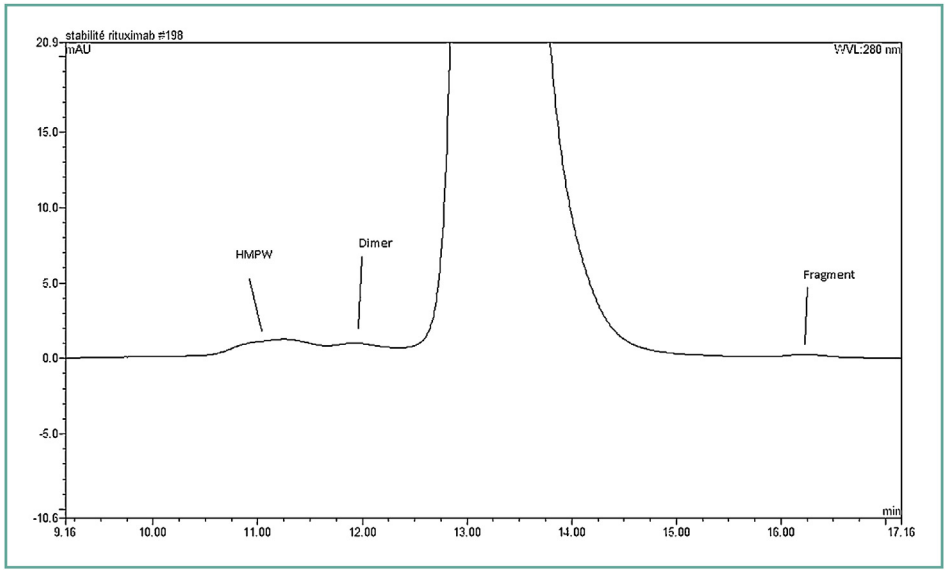

Figure 6. Magnification of a typical SEC chromatogram showing the dimer and HMW peaks.
Agrandissement d'un chromatogramme SEC typique montrant les pics de dimère et de haut poids moléculaires.

Table 5 Relative percentages for the SEC peaks (bags with two concentrations of the rituximab biosimilar), at T0 and on D28 for 2 temperatures. No significant difference was observed after 28 days of storage.
Pourcentage relatifs des pics en SEC (poches à 2 concentrations du biosimilaire de rituximab) à T0 et après 28 jours à 2 températures. Aucune différence significative a été observée après 28 jours de stockage.

		C1 (1 mg/mL)						C2 (4 mg/mL)					
		4 °C			25 °C			4 °C			25 °C		
	Peak no./ Batch	1	2	3	1	2	3	1	2	3	1	2	3
T0	1	0.30	0.29	0.33	0.26	0.29	0.32	0.28	0.28	0.31	0.27	0.28	0.31
	2	0.09	0.10	0.09	0.10	0.10	0.09	0.09	0.10	0.10	0.10	0.10	0.09
	3	99.53	99.53	99.49	99.55	99.52	99.50	99.54	99.54	99.51	99.55	99.53	98.92
	4	0.09	0.08	0.08	0.09	0.09	0.09	0.09	0.08	0.09	0.09	0.09	0.68
D28	1	0.29	0.27	0.31	0.07	0.07	0.07	0.29	0.27	0.30	0.02	0.23	0.24
	2	0.08	0.09	0.08	0.32	0.30	0.24	0.09	0.10	0.09	0.21	0.10	0.09
	3	99.54	99.56	99.52	99.52	99.53	99.59	99.54	99.56	99.52	99.67	99.52	99.10
	4	0.08	0.07	0.08	0.09	0.10	0.09	0.09	0.08	0.09	0.09	0.15	0.57

observed as a function of storage conditions remained minimal and were within the range of inter-batch variability [24]. However, these variations are difficult to explain. The decrease in monomer content of the vials may be consistent with dimerization or oligomerization with increasing antibody concentration. However, the corresponding peaks did not increase significantly, although there was a tendency in this direction. The low levels of these compounds may also be responsible for imprecision in peak integration.

Nevertheless, after dilution and storage at 25 °C for 28 days, the rituximab biosimilar showed no marked sign of oligomer formation.

DLS analyses

DLS was used to study the hydrodynamic properties of the monomer, diameter and dispersity, to search for submicron populations reflecting intramolecular nucleation phenomena, to obtain thermal aggregation curves and to determine melting point (Tm or Tagg).

Hydrodynamic diameter and submicron populations

Mean hydrodynamic diameter at T0 for a concentration of 1 mg/mL was 11.24 ± 0.073 nm, with a dispersity of 0.071 ± 0.010. For a concentration of 4 mg/mL, mean hydrodynamic diameter was 11.67 ± 0.10 nm with a dispersity index (DI) of 0.074 ± 0.007. The hydrodynamic diameter at a concentration of 4 mg/mL was significantly larger than that at 1 mg/mL ($P < 0.0001$; Student's *t*-test). No significant differences were found between the three batches tested. This diameter is highly consistent with that determined during our previous study on the stability of Mabthera® rituximab (11.18 ± 0.24 nm) [10]. We observed no difference as a function of storage temperature or batch between T0 and D28, for either concentration (Anova: $P = 0.0748$; Student-Newman-Keuls multiple comparison test: non-significant for all comparisons). The very low dispersity index values obtained suggest that no dimerization occurred and are highly consistent with the SEC results, although this method may disrupt weak associations between molecules.

No change in hydrodynamic diameter or dispersity was observed during storage (Table 6).

For the vials (10 mg/mL), mean hydrodynamic diameter was higher, for all three batches, than for the diluted solutions (12.76 ± 0.049 nm; $P < 0.001$). After 28 days of storage at 4 °C, hydrodynamic diameter had not changed (12.86 ± 0.177 nm; non-significant difference relative to T0). By contrast, following storage at 25 °C, we noted a very slight increase (13.49 ± 0.360 nm; $P < 0.05$). No change in dispersity index was observed. A linear relationship was found between the hydrodynamic diameter and the protein concentration ($r = 0.9969$). This slight increase in hydrodynamic diameter between concentrations may be due to concentration-dependent labile dimerization, even though this phenomenon was not detected on SEC. It remains possible that weak links form between monomers, leading to an increase in hydrodynamic diameter, but that these links can be destroyed during chromatographic analysis, like artifacts linked to changes in viscosity due to higher protein concentration. As a more pertinent indicator of physical stability, we did not observe the appearance of populations with a larger hydrodynamic diameter, in the 100 to 1000 nm range, in particular. These results demonstrate the absence of a phenomenon of nucleation likely to lead to aggregate formation. They are highly consistent with the turbidimetry results.

We can therefore conclude that the storage of the rituximab biosimilar for a month, at 4 °C or 25 °C, has no effect on its hydrodynamic diameter (other than a very slight effect for vials stored at 25 °C) and does not trigger the formation of populations of submicron aggregates.

Thermal aggregation curve

We used DLS to estimate possible changes in the thermodynamic resistance of the rituximab biosimilar during its storage in solution, by establishing temperature-dependent aggregation curves and determining the melting point (Tm), which is characteristic of the protein. We obtained a mean

Table 6 Hydrodynamic diameters and dispersity index (DI) for the bags (3 batches).
Diamètres hydrodynamiques et index de dispersité (DI) pour les poches (3 lots).

		C1 (1 mg/mL)						C2 (4 mg/mL)					
		4 °C			25 °C			4 °C			25 °C		
	Batch no.	1	2	3	1	2	3	1	2	3	1	2	3
TO	Diameter (nm)	11.20	11.33	11.29	11.12	11.26	11.24	11.59	11.64	11.69	11.55	11.79	11.77
	SD	0.13	0.10	0.03	0.03	0.03	0.03	0.05	0.09	0.05	0.06	0.02	0.06
	DI	0.071	0.088	0.092	0.063	0.077	0.076	0.053	0.059	0.063	0.050	0.072	0.063
	SD	0.010	0.021	0.003	0.009	0.012	0.011	0.004	0.016	0.004	0.009	0.008	0.010
D28	Diameter (nm)	11.25	11.29	11.49	11.34	11.30	11.24	11.47	11.46	11.52	11.39	11.43	11.50
	SD	0.05	0.04	0.08	0.16	0.05	0.02	0.05	0.06	0.08	0.05	0.06	0.03
	DI	0.084	0.088	0.123	0.099	0.091	0.095	0.056	0.055	0.061	0.059	0.060	0.081
	SD	0.011	0.002	0.034	0.012	0.011	0.013	0.010	0.003	0.014	0.010	0.006	0.011

Table 7 Melting points at D28 (Tm, expressed in °C ± SD) of the rituximab biosimilar CT-P10 determined by DLS (3 batches for 2 dilutions in bags and 10 mg/mL vials). The mean initial value was 71.79 ± 0.10 °C.
Points de fusion à 28 jours (Tm, exprimé en °C ± SD) du biosimilaire de rituximab CT-P10, déterminés par DLS (3 lots pour 2 dilutions en poches et les flacons à 10 mg/mL). La valeur moyenne initiale était de 71,79 ± 0,10 °C.

	4 °C						25 °C								
	C1			C2			C1			C2			Vials		
Batch no.	1	2	3	1	2	3	1	2	3	1	2	3	1	2	3
Mean	72.18	71.14	71.24	72.16	72.11	72.05	71.95	71.38	71.67	71.81	71.81	ND	72.06	72.03	71.41
± SD	0.11	0.14	0.11	0.10	0.10	0.00	0.22	0.12	0.29	0.22	0.04	ND	0.21	0.05	0.03

The mean initial value was 71.79 + 0.10 °C. ND: not determined. No significant difference was observed as compared to the mean initial value.

value of 71.79 ± 0.10 °C, which is consistent with the value reported in a previous study by our team (72.5 ± 0.29 °C). The Tm values obtained were not dependent on concentration, consistent with a weak quinary structure. As shown in Table 7, for each concentration, there was no difference between batches, temperatures or storage times (Anova: $P = 0.893$ for C1 and $P = 0.276$ for C2; Student-Newman-Keuls multiple comparison test: non-significant for all comparisons). In conclusion, we observed no effect of storage duration or temperature on the tendency of the rituximab biosimilar to aggregate. Thermodynamic stability does not seem to be affected by concentration, temperature or storage duration.

SEC study of quinary structure

The measurement of retention time on SEC as a function of the concentration of a protein in solution (injection-dilution SEC) can be used to assess quinary structure. This approach can thus be used to estimate the tendency of a protein to form stable oligomers. Fig. 7 shows the results for the study of quinary structure for the rituximab biosimilar. The very little variation in retention time (13.267 min at 0.05 mg/mL; 13.195 min at 10 mg/mL) and the very slow rate of decrease of the corresponding RT = f(conc) curve fitted to a linear model (first-order rate constant: −0.0067 °C per mg/mL) are entirely consistent with the results reported by Chen et al. [21], confirming the weak tendency of the biosimilar to form stable oligomers. These results validate the use of the SEC method for estimating the tendency to form stable oligomers and aggregates at the opposite of DLS since the previously demonstrated concentration-dependant hydrodynamic diameter relationship showed a tendency to labile dimerization. The dilution of the sample has no significant effect on the likelihood of detecting dimers or oligomers.

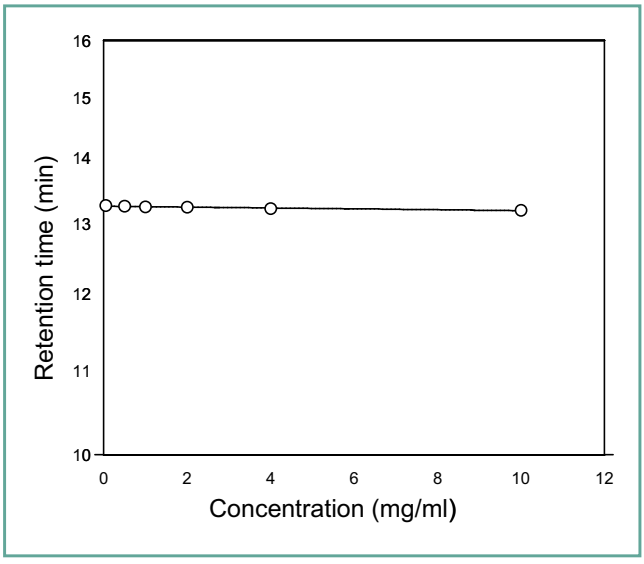

Figure 7. SEC retention time vs. concentration of injected RTX biosimilar (0.05 to 10 mg/mL). The data were fitted to a linear model.
Temps de rétention de SEC vs la concentration injectée du biosimilaire de RTX (0,05 à 10 mg/mL). Les donnés sont mises en un modèle linéaire.

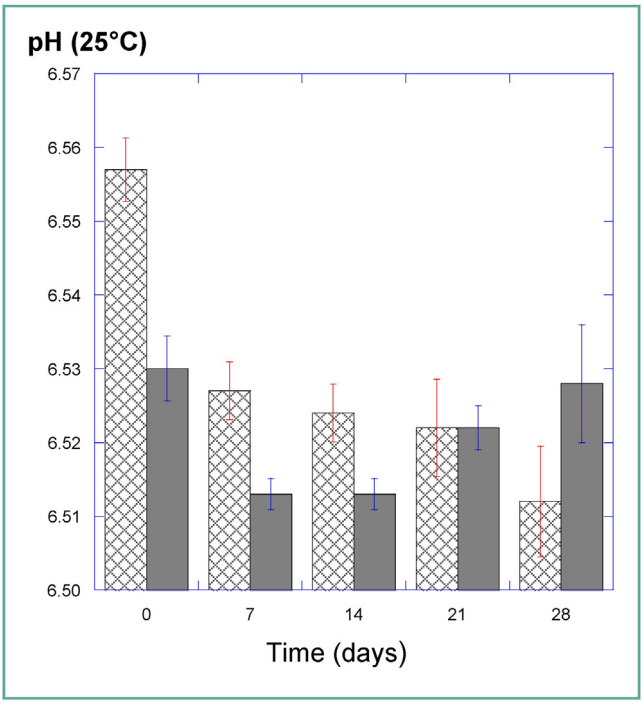

Figure 8. Changes in pH (corrected at 25 °C) of the rituximab biosimilar solutions as a function of storage time (mean ± SD; grey bars: vials, hatched bars: bags).
Modifications du pH (corrigé à 25 °C) du biosimilaire de rituximab en fonction de la durée de stockage (moyenne SD ; barres grises : flacons ; barres hachurées : poches).

These results are also highly consistent with the DLS results, which showed an absence of submicron aggregate population formation during storage.

General parameters: density, pH and osmolarity

Density

The oscillating U-tube method yielded a density value at T0 of 1.0047 ± 0.0003 g/mL for the 1 mg/mL bags, 1.0075 ± 0.0002 g/mL for the 4 mg/mL bags, and 1.0112 ± 0.0003 g/mL for the 10 mg/mL vials. No significant change in density was observed after 28 days of storage, for any of the conditions tested.

pH

We observed a rapid decrease in pH beginning on D7 (6.557 ± 0.004 at T0 and 6.527 ± 0.004 at D7), which then became more gradual and continued until D28 for the bags. This decrease in pH was interpreted as the result of acidification due to the diffusion of CO_2 into the bags. The initial pH of the vials was slightly lower (6.530 ± 0.004), with a decrease beginning on D7 followed by an increase in pH back to its initial value on D28 (Fig. 8). However, these changes remained very modest (< 0.05 pH units) and had no effect on stability.

Osmolarity

For concentration C1, osmolarity was 287.5 ± 1.2 mOsmol at T0, and 289.2 ± 0.98 mOsmol after 28 days of storage, with no significant differences between D0, D7, D14, D21 and D28 (Kruskal-Wallis test; $P = 0.0578$; NS) regardless of the storage temperature.

For concentration C2, osmolarity was, as expected, higher than for C1: 312.3 ± 3.14 mOsmol at T0, with no significant change until D28 (311.3 ± 1.36 mOsmol).

For vials, the initial osmolarity was 356.3 ± 1.50 mOsmol, consistent with the 10 mg/mL concentration of the protein. It reached 359.3 ± 2.31 mOsmol after 28 days of storage at 4 °C (non-significant difference relative to T0) and 362.3 ± 1.57 mOsmol after 28 days of storage at 25 °C. This increase in osmolarity in the vials remains unexplained.

Sterility study

No bacterial contamination was detected in any of the samples, despite the lack number of samples taken for analytical purposes. These results show that the samples were initially sterile and that the successive samples did not lead to the introduction of contamination that could have led to artifacts in the analytical determinations carried out. They confirm that, provided that manipulations of rituximab biosimilar vials are performed in sterile conditions, the stability parameters are essentially physicochemical.

Search for large particles

The microscopic image analysis showed no significant differences in particle levels after 28 days, regardless of the concentration and storage temperature.

Conclusion

The stability of the rituximab biosimilar CT-P10 marketed by Laboratoires Biogaran, in 50 mL vials at a concentration of 10 mg/ml, and after dilution to final concentrations of 1 and 4 mg/mL and storage in polyolefin bags at 4 °C and 25 °C was studied by several orthogonal and complementary methods. No significant change (as defined by a magnitude greater than the inter-batch variability) [24] was observed, for each of the parameters characterizing physical and chemical stability studied, for the two concentrations and temperatures tested, or for any of the three batches tested.

Vials at 10 mg/mL after opening and diluted bags at 1 and 4 mg/mL in NaCl, stored for 28 days at 4 °C or 25 °C, displayed no sign of physical instability relative to freshly prepared bags: they contained no submicron or micro-size aggregates and no particles. Size-exclusion chromatography profiles revealed no formation of dimer and oligomer or disruption of the molecular structure. Ion-exchange chromatography showed no significant change in the distribution of ionic variants, indicating an absence of change to the initial structure, with, in particular, no sign of deamidation or deglycanation. Spectral analysis by derivative UV and fluorescence spectroscopy revealed no change, particularly as concerned the tertiary structure of the antibody, during storage at 4 °C for 28 days. By contrast, signs of modification to the tertiary structure of the molecule were observed, but only after storage at 25 °C for 28 days. The thermal denaturation curves were identical, suggesting an absence of thermodynamically permanent destabilization of the global high-order structure.

No biological activity was determined. Indeed, our previous study on the stability of the original rituximab molecule (Mabthera®) showed that, after six months of storage of the diluted solution at 4 °C, cytotoxic activity was completely maintained [10]. There is therefore no reason to think, given very comparable quality attributes [23] and the excellent physicochemical stability of the biosimilar demonstrated in the present study, that its biological activity might be significantly altered after 28 days of storage at 4 °C.

It can, therefore, be concluded that, after dilution in sterile conditions, with 0.9% NaCl, in polyolefin bags, to the concentrations routinely used (1 and 4 mg/mL), the rituximab biosimilar CT-P10 appears to remain stable for at least one month in complete darkness at 4 °C. After 28 days of storage at 25 °C, only the tertiary structure of the molecule appeared to be slightly altered, with no marked changes in terms of aggregate formation of chemical alterations. The same conclusions can be drawn for the vials of undiluted product. However, this alteration was not observed after 15 days at the same temperature.

From a practical point of view, our results demonstrate that opened vials of the RTX biosimilar CT-P10 can be kept at room temperature for several days (up to 15 days) without significant degradation. This fact is of crucial importance for users in case of temperature excursion such as failure of fridge during the week-end or bad transportation conditions, and obviously also for unopened vials. Since the biosimilar RTX in opened vials is stable at 4 °C up to one month, residues can also be used after to avoid any loss of this expensive drug. The same reasoning can be applied to the bags of the diluted biosimilar. This implies that an advance preparation is safely feasible to avoid unnecessary delays in the management of the patient and improvement of the pharmacy and nurse workload. The excellent stability can also permit dose-banding or eventually the use of a flat-dose, leading to preparation by batch assuring a complete quality control. Obviously, this extended stability can only be ensured if validated adequate aseptic techniques are applied throughout the manufacturing and storage processes.

Finally, if our results could be incorporated by the manufacturer into the SPC of this biosimilar, they could bring an interesting added value for an optimal decision to introduce it into a hospital therapeutic formulary.

Acknowledgments

The authors express their thanks to Biogaran laboratories for their generous financial support and the gift of biosimilar vials.

Disclosure of interest

The authors declare that they have no competing interest.

References

[1] Cheung MC, Haynes AE, Meyer RM, Stevens A, Imrie KR. Rituximab in lymphoma: a systematic review and consensus

practice guideline from Cancer Care Ontario. Cancer Treat Rev 2007;33:161—76.
[2] Edwards JC, Szczepanski L, Szechinski J, Filipowicz-Sosnowska A, Emery P, Close DR, et al. Efficacy of B-cell-targeted therapy with rituximab in patients with rheumatoid arthritis. N Engl J Med 2004;350:2572—81.
[3] Pedersen IM, Buhl AM, Klausen P, Geisler CH, Jurlander J. The chimeric anti-CD20 antibody rituximab induces apoptosis in B-cell chronic lymphocytic leukemia cells through a p38 mitogen activated protein-kinase-dependent mechanism. Blood 2002;99:1314—9.
[4] Manning MC, Chou D, Murphy BM, Payne RW, Katayama DS. Stability of protein pharmaceuticals: an update. Pharm Res 2010;27:544—75.
[5] Wang W. Instability, stabilization, and formulation of liquid protein pharmaceuticals. Int J Pharm 1999;185:129—88.
[6] Chi EY, Krishnan S, Randolph TW, Carpenter JF. Physical stability of proteins in aqueous solution: mechanism and driving forces in nonnative protein aggregation. Pharm Res 2003;20:1325—36.
[7] Wang W, Singh S, Zeng DL, King K, Nema S. Antibody structure, instability, and formulation. J Pharm Sci 2007;96:1—26.
[8] Wakankar AA, Borchardt RT. Formulation considerations for proteins susceptible to asparagine deamidation and aspartate isomerization. J Pharm Sci 2006;95:2321—36.
[9] Bardin C, Astier A, Vulto A, Sewell G, Vigneron J, Trittler R, et al. Guidelines for the practical stability studies of anticancer drugs: a European consensus conference. Ann Pharm Fr 2011;69:221—31.
[10] Paul M, Vieillard V, Jaccoulet E, Astier A. Long-term stability of diluted solutions of the monoclonal antibody rituximab. Int J Pharm 2012;436(1—2):282—90.
[11] Sreedhara A, Glover ZK, Piros N, Xiao N, Patel A, Kabakoff B. Stability of IgG1 monoclonal antibodies in intravenous infusion bags under clinical in-use conditions. J Pharm Sci 2011;101:21—30.
[12] Bardo-Brouard P, Vieillard V, Shekarian T, Marabelle A, Astier A, Paul M. Stability of ipilimumab in its original vial after opening allows its use for at least 4 weeks and facilitates pooling of residues. Eur J Cancer 2016;58:8—16.
[13] Paul M, Vieillard V, Da Silva Lemos R, Escalup L, Astier A. Long-term physico-chemical stability of diluted trastuzumab. Int J Pharm 2013;448(1):101—4.
[14] Mahler HC, Muller R, Friess W, Delille A, Matheus S. Induction and analysis of aggregates in a liquid IgG1-antibody formulation. Eur J Pharm Biopharm 2005;59:407—17.
[15] Hawe A, Kasper JC, Friess W, Jiskoot W. Structural properties of monoclonal antibody aggregates induced by freeze-thawing and thermal stress. Eur J Pharm Sci 2009;38(2):79—87.
[16] Servillo L, Colonna G, Balestrieri C, Ragone R, Irace G. Simultaneous determination of tyrosine and tryptophan residues in proteins by second-derivative spectroscopy. Anal Biochem 1982;126:254—7.
[17] Balestrieri C, Colonna G, Giovane A, Irace G, Servillo L. Second-derivative spectroscopy of proteins: studies on tyrosyl residues. Anal Biochem 1980;106:49—54.
[18] Harn N, Allan C, Oliver C, Middaugh CR. Highly concentrated monoclonal antibody solutions: direct analysis of physical structure and thermal stability. J Pharm Sci 2007;96(3):532—46.
[19] Vieillard V, Astier A, Sauzay C, Paul M. One-month stability study of a biosimilar of infliximab (Remsima®) after dilution and storage at 4 °C and 25 °C. Ann Pharm Fr 2017;75:17—29.
[20] Farruggia B, Garcia G, D'angelo C, Pico G. Destabilization of human serum albumin by polyethylene glycols studied by thermodynamical equilibrium and kinetic approaches. Int J Biol Macromol 1997;20:43—51.
[21] Chen K, Long DS, Lute SC, Levy MJ, Brorson KA, Keire DA, et al. methods for evaluating higher order structures of monoclonal antibody therapeutics with quinary structure. J Pharm Biomed Anal 2016;128:398—407.
[22] Pan B, Maciejewski MW, Marintchev A, Mullen GP. Solution structure of the catalytic domain of gamma delta resolvase. Implications for the mechanism of catalysis. J Mol Biol 2001;310:1089—107.
[23] Visser J, Feuerstein I, Stangler T, Schmiederer T, Fritsch C, Schiestl M. Physicochemical and functional comparability between the proposed biosimilar rituximab GP2013 and originator rituximab. BioDrugs 2013;27:495—507.
[24] Schiest M, Stangler T, Torella C, Čepeljnik T, Toll H, Grau R. Acceptable changes in quality attributes of glycosylated biopharmaceuticals. Nature Biotech 2011;29:310—2.